Constant-pH Molecular Dynamics with Ionic Strength Effects: Protonation−Conformation Coupling in Decalysine

Miguel Machuqueiro and António M. Baptista*

Instituto de Tecnologia Química e Biológica, Universidade Nova de Lisboa, Av. da República, EAN, Apartado 127, 2781-901 Oeiras, Portugal

Received: November 8, 2005; In Final Form: December 15, 2005

A new implementation of the stochastic titration method for constant-pH molecular dynamics is presented, which introduces ionic strength effects in the simulations. In addition, the new implementation uses a faster molecular dynamics algorithm and an improved treatment of protonation events and of their effect on force field parameters. This new methodology is applied to a decalysine peptide, yielding very good quantitative agreement with experiments, both in terms of titration and helix-coil transition. The results show a significant dependence on ionic strength, illustrating the importance of including this parameter in constant-pH molecular dynamics simulations. Overall, the method seems to properly capture the protonation−conformation coupling and its dependence on ionic strength.

Introduction

All living things are water-based systems, meaning that they depend heavily on aqueous equilibria, especially acid−base equilibrium. The pH dependence of protein structure and function is thus an important issue, well established for quite some time.[1] pH effects occur via electrostatic interactions, one of the strongest forces at molecular level, and can have a direct influence on molecular structure, as dramatically illustrated by protein denaturation at extreme pH values. However, the coupling between protonation and conformation can be much more subtle, as recently illustrated by the protein misfolding process implicated in a large number of pathologies.[2−4] In many of these cases, small pH changes can result in small changes in the charge of the protein, which in turn induce conformational transitions leading to amyloid plaque aggregation and disease. These cases strengthen the importance of gaining a detailed understanding of protonation−conformation coupling and the way it is affected by pH.

In terms of computational studies, pH effects on proteins have been investigated using different and somewhat complementary approaches. Standard molecular mechanics/dynamics (MM/MD) simulations can deal with pH in a rather limited way, usually by setting the protein protonable groups to the states they would have in a solution at the intended pH. This means that any desolvation and site−site interaction effects caused by the protein environment are entirely neglected. Another approach resorts to rigid protein structures and simplified electrostatic-oriented models, such as Poisson−Boltzmann (PB),[5−10] generalized Born (GB),[11,12] or protein dipoles and Langevin dipoles (PDLD).[13,14] The protonation free energies thus obtained can then be used for sampling protonation states by Monte Carlo (MC)[8,15−17] or other approximate methods,[8,13,18−21] making possible the calculation of pK_a values. These approaches explicitly consider the effect of desolvation and site−site interactions, but the use of a single protein conformation makes impossible to account for structural reorganization and protonation−conformation coupling in general.[22−25] Clearly, MM/MD simulations and simplified models are largely complementary with respect to the treatment of conformation and protonation: MM/MD samples conformations at fixed protonation, while simplified models sample protonation at fixed conformation. Another route to address pH effects in proteins is to compute protonation free energies using the standard thermodynamic integration and perturbation methods,[26,27] although at a high computational cost. An alternative, which combines MM/MD with simplified models, is the use of linear response approximation (LRA) methods, where MM/MD-sampled conformations are used for protonation calculations with PDLD-type[13,14,24,28] or PB[22,29] models. These LRA methods combine the speed of simplified models with the explicit consideration of conformation flexibility, being quite effective in dealing with structural reorganization.

A recent alternative to study pH effects is the use of constant-pH MD methods, where pH plays the role of an external parameter like the temperature or pressure and whose effect is reflected on the resulting sample of conformations and protonation states. The first attempt in this direction was done by Mertz and Pettitt,[30] who applied their extended-system grand-canonical MD method to the reaction of proton exchange between acetic acid and water. A different approach, exploring the complementarity between MM/MD and simplified models, was followed in our implicit titration method for constant-pH MD,[31] which uses fractional protonation states periodically updated from PB/MC calculations performed along the MD simulation. The method is based on a potential of mean force which ensures that it samples from the proper semi-grand canonical ensemble. Although the original implementation resorted to a mean field approximation and a PB method with little atomic detail, the implicit titration method efficiently combines these two approaches and allows them to do what they do best: MM/MD does the conformation sampling at fixed protonation state, and PB/MC does the protonation sampling at fixed conformation. Following a similar rationale of complementarity, we proposed also a stochastic titration method for constant-pH MD,[32] where discrete (nonfractional) protonation

* To whom correspondence should be addressed. Tel.: +351 214469619. Fax: +351 214411277. E-mail: baptista@itqb.unl.pt.

10.1021/jp056456q CCC: $33.50
Published on Web 01/27/2006

states are similarly obtained from periodic PB/MC calculations. The coupling between the MM/MD and PB/MC algorithms ensures a proper Markov chain sampling from the semi-grand canonical ensemble. Similar stochastic constant-pH MD methods were proposed by Antosiewicz and co-workers[33−35] and by Mongan et al.;[36] the main differences are the overall use of implicit solvation models (uniform-dielectric Langevin dynamics,[33] analytical continuum solvent potential,[34,35] and GB[36]) in the MD simulations and the replacement of the PB model by GB in one of the methods.[36] A different route, not based on simplified models, was followed by Bürgi et al.,[37] who proposed a method where short segments of MM/MD thermodynamic integration are used to compute the free energies of trial Monte Carlo changes of the protonation states. This constant-pH MD method has a high computational cost, and the sampling efficiency of the short free energy calculations is questionable. The acidostat method proposed by Börjesson and Hünenberger[38,39] is also entirely based on MM/MD. The method uses fractional protonation states weakly coupled to a proton bath, but its theoretical basis is problematic.[40] Another constant-pH MD method using continuous titration coordinates was recently proposed by Brooks and co-workers.[41,42] The method uses a GB implicit solvent model and is based on heuristic analogies with λ-dynamics[43] and LRA.

Electrostatic interactions, and consequently pH effects, can be significantly affected by ionic strength. The possibility of including ionic strength effects in constant-pH MD depends on the characteristics of the method being used. Here we will discuss only the inclusion of ionic strength effects in the stochastic titration method,[32] although much of the discussion is also relevant for the other methods. The inclusion of ionic strength in the calculation of each new protonation state is straightforward, because it can be directly included in the PB calculations. The inclusion of ionic strength in the MM/MD segments is more problematic and has been the subject of some studies using standard MM/MD. In a study using particle mesh Ewald (PME) to treat electrostatic interactions, Ibragimova and Wade[44] found that, to obtain stable structures, the MD simulations required an amount of counterions corresponding to the ionic strength of the solution, in addition to a minimal set of neutralizing counterions. Furthermore, while comparing lattice-sum and reaction-field methods, Walser et al.[45] found that the inclusion of counterions was indeed advantageous with the lattice-sum method but not with the reaction-field method; overall, the performances of the lattice-sum simulations with counterions and of the reaction-field simulations without counterions were very similar, with a slightly better performance for the latter. The inclusion of counterions in the stochastic titration method is problematic because the total charge of the system is changing during the simulation. Therefore, and considering the studies just mentioned, the use of the reaction field method without counterions seems the most convenient route in this case. Furthermore, the generalized reaction field method allows for the specification of the ionic strength, which results in a further screening effect.[46] Thus, the constant-pH stochastic titration method can include the effect of ionic strength by specifying its value at two levels: (1) in the PB calculations; (2) in the generalized reaction field used in the MD segments. This will be the approach used in this work.

The principles involved in pH-induced structural changes in proteins can be investigated by the study of model systems. Poly-L-lysine has been used for that purpose for quite some time, since it displays a clear conformational transition between α-helix and random-coil upon pH changes.[47] At high pH ($\gg$10.3) poly-L-lysine is mostly neutral (i.e., deprotonated), adopting an α-helical conformation. At low pH ($\ll$10.3) the lysine side chains become mainly charged (i.e., protonated), leading to higher repulsion and consequently to the destabilization of the helix and the predominance of random-coil. Around pH 10.3, the system is in equilibrium between α-helix and random-coil. A decalysine peptide was previously used in the context of constant-pH MD by Börjesson and Hünenberger.[39] These authors applied their acidostat method to decalysine and reproduced the general experimental trend of the helix−coil transition. However, their results indicate that half-protonation takes place around pH 9.0, one unit below the experimental value. As for the midpoint of the helix−coil transition, the data provided does not allow for a simple quantitative estimation, but analysis of the secondary structure plots in Figures 5−8 of ref 39 suggests that it occurs around pH 9.5, again below the experimental value of 10.3. As noted by the authors, the discrepancies may result from the fact that the experimental data refer to an ionic strength of 0.1 M, while no attempt to include such effects were done in the acidostat simulations (analysis of the article where the method was originally proposed[38] suggests that this would imply reparametrizing the auxiliary function $F(\lambda)$ at different ionic strength values).

In this work we use constant-pH MD simulations to investigate in detail the helix−coil transition of decalysine and its dependence on ionic strength. We use the stochastic titration method previously described,[32] including counterion effects as outlined above. This also allows us to apply the stochastic titration method to a system considerably larger than the succinic acid molecule originally used as a test system.[32]

Computational Details and Methods

Constant-pH MD Method. The method implemented is the constant-pH MD method using stochastic titration, previously proposed.[32] The current implementation differs from the previous one in the following: MM/MD is now performed using the GROMACS package,[48] which allows for a 5-fold increase in MD speed; the force-field files were modified to get a better interface between PB/MC and MD. This last modification, together with the topology generation on-the-fly, allows that a protonation/deprotonation results in a change, not only of the partial charges (as previously[32]) but also of the atom types, bond distances, angles, and dihedrals.

The PB and MC calculations were done, as in the previous implementation,[32] using the programs MEAD[49] and MCRP,[17] respectively. The atomic charges and radii used in the PB calculations were derived from the 53A6 force field of the GROMACS distribution.[48] All PB calculations consisted of finite-difference linear Poisson−Boltzmann calculations performed with the program MEAD (version 2.2.0),[49] using a temperature of 300 K, a molecular surface defined with a solvent probe radius of 1.4 Å, and a Stern (ion exclusion) layer of 2.0 Å. The dielectric constants were 2 for decalysine and 80 for the solvent. A two-step focusing procedure[50] was used, with consecutive grid spacings of 1.0 and 0.25 Å. MC runs were performed using 10^5 MC cycles, one cycle consisting of sequential state changes over all individual sites and also all pairs of sites with at least one interaction term above 2.0 pK_a units.[17]

The algorithm used (Scheme 1) in this work is very similar to the one previously published,[32] diverging mainly in the extra conditional loop we added for *reduced titration*. This reduced titration approach is a variation of the reduced titration method introduced by Bashford and Karplus;[21] in our variation we run

SCHEME 1. Schematic Representation of the Algorithm Used

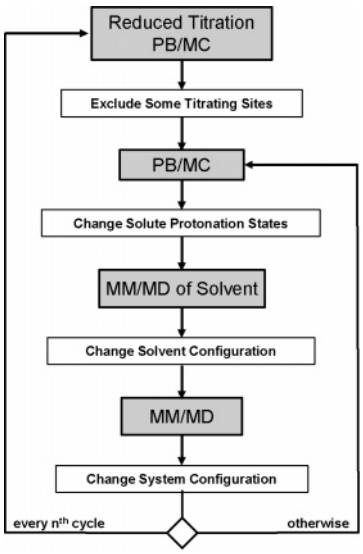

a full PB/MC calculation on the system every *n*th step to assign a fixed state to all the sites whose mean occupancies fall outside a predefined threshold (see below).

As previously, this method relies on different sequential blocks. The first block is a PB/MC calculation which is applied only to the relevant titrable sites (as selected by reduced titration; see below). The protonation states resulting from the last MC step are assigned to the protein. The second block is the solvent relaxation dynamics, a short MM/MD simulation of the system with frozen protein, which allows the solvent to adapt to the new protonation states (the duration of this block is hereafter designated as τ_{rlx}). The last block is a full MM/MD of the unconstrained system (the duration of this block is hereafter designated as τ_{prt}).

Reduced Titration. With the reduced titration we intended to create an exclusion list with sites that are titrating too far away from the pH we are interested in. The method needs two parameters: the step interval (10 cycles = 20 ps, in our simulations), which is the time between updates of the list; the exclusion threshold (0.01, in this work), which is a value between 0 and 1 that defines the minimum/maximum (0.01/ 0.99) occupancy for a site to be out of the exclusion list (note that if the threshold is 0, the reduced titration cycle will be bypassed). The implementation of the reduced titration method not only speeds the simulations but also automatizes the process of setting simulations at different pH values.

MM/MD Settings. All simulations were performed with the GROMOS 53A6 force field[51] for the GROMACS distribution and with the SPC water model.[52] Periodic boundary conditions were used, with a dodecahedral unit cell. Nonbonded interactions were calculated using a twin-range cutoff, with short- and long-range cutoffs of 8 and 14 Å, respectively. Long-range electrostatics interactions were treated using the generalized-reaction-field method,[46] where we could change the value of the ionic strength. The official release of GROMACS 3.2.1 has a bug in the code leading always to an ionic strength of zero. To bypass this problem, we changed the code so that the software could treat the ionic strength as an external parameter like the temperature. All bond lengths were constrained using the LINCS algorithm[53] which allowed the use of a time step of 2 fs. Two Berendsen's[54] temperature couplings to baths at 300 K and relaxation times of 0.1 ps were used for both the solute and solvent. A Berendsen's pressure coupling[54] was used to scale the box, using a relaxation time of 0.5 ps and a compressibility of 4.5×10^{-5} bar^{-1}. For some of test simulations with counterions (see below) we used PME[55] to treat the long-range electrostatics interactions. A grid spacing of 0.12 nm was used, and the short-range interactions were calculated using a nonbond pairlist with a single cutoff of 0.9 nm.

The decalysine polymer was built in an α-helix conformation and capped at both termini using an amino group at the C-terminus and an acetyl group at the N-terminus. The peptide was placed at the center of a box, which was filled with 4406 water molecules. The counterions Na^+ and Cl^- were added according to the electrostatic potential using the *genion* tool available in GROMACS.

The system was minimized first with ~40 steps of steepest descent followed by ~700 steps using the l-bfgs (low-memory Broyden−Fletcher−Goldfarb−Shanno) algorithm. The initiation was achieved by harmonically restraining all protein atoms in a 50 ps MD simulation, followed by another 50 ps simulation with only the CA atoms restrained. This initiation was done for both the fully protonated and the fully deprotonated forms. The charged conformation was used as the starting structure for the simulations at pH 7.0, 8.5, and 9.5, while those at pH 10.3 and 11.5 were started with the neutral conformation.

Runs of 20 ns were performed. Equilibrium is generally achieved after the first 5 ns, which were discarded in data analysis. The relaxation of the solvent (τ_{rlx}) was done for 0.2 ps while each full system dynamics segment (τ_{prt}) was 2.0 ps long. If τ_{prt} is too short, the system may become trapped at a particular protonation/deprotonation interface in phase space and the computational cost increases; if it is too long, we may get a too slow conformational sampling. In this work, the τ_{rlx} and τ_{prt} values were optimized to get low computational cost (only 9% of the MM/MD time is "wasted" in relaxing the solvent), good system stability, and reasonable conformational sampling.

Analysis. Secondary structure assignment was done using the DSSP program by Kabsch and Sander.[56] Other structural analyses were done using GROMACS[48] or in-house tools. The calculation of correlation-corrected errors for averages were computed using standard methods.[57]

Results and Discussion

Titration with Constant-pH MD. The titration of decalysine was computed by averaging the occupancy states of all lysines over 15 ns of simulation for each pH value. These simulations were done for two different values of ionic strength (0.0 and 0.1 M) and compared with the results of Chou and Scheraga.[47] The experimental titration curve refers to poly-L-lysine with a chain length of ~670 units in a 0.1 KCl solution at 298 K and was determined using potentiometric titration.

From our results (Figure 1), we observe that at 0.1 M our curve is less sigmoidal than the experimental one. This difference can be accounted by the strong coupling between protonation and conformation and therefore depends on the conformation transition curves (see below). Nevertheless, the difference between experimental and simulation curves is small and within the error range. The pH at half-protonation (~9.8) is reasonably close to the experimental one (~10). There is a clear effect of the ionic strength on the titration curve. At ionic strength of 0.0 M, we observe pH shifts as high as one unit for the same protonation values. This shift occurs toward the acidic direction due to electrostatic effects. In fact, at lower ion concentration, the repulsion between the positively charged lysine residues is enhanced, which renders protonation more difficult. When comparing our results at ionic strength 0.0 M

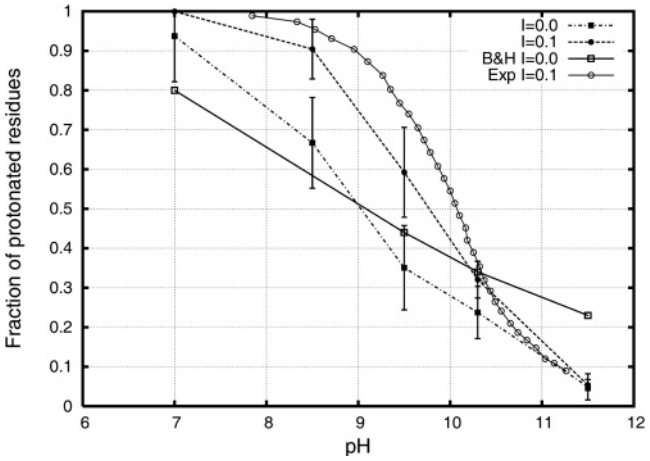

Figure 1. Titration curves at two different ionic strengths compared with the experimental one (I = 0.1 M KCl)[47] and the results from Börjesson and Hünenberger.[39]

with the titration curve from Börjesson and Hünenberger,[39] we note good agreement between the pH values at half-protonation. This result is not entirely surprising because, as noted in the Introduction, the acidostat method from these authors does not take into account the effect of ionic strength.

Nonhelical Structures and Reversibility. Our main approach to study the helicity of decalysine was to use the secondary structure assignment of the DSSP program.[56] The helical quantification was obtained by summing the π-helix, α-helix, and 3_{10}-helix contents in decalysine. It is important to mention that both π- and 3_{10}-helices occur rarely in the simulations and only reflect fluctuations in the α-helix structure rather than a structure transition. For this analysis, we ignored the first and last lysine residues, due to the fact that they are very mobile and not very descriptive of the overall structure.

Figure 2 shows two plots of the number of residues in helical conformation over time at pH 8.5 and 11.5 and at ionic strength 0.0 M. The fact that during a few nanoseconds the decalysine showed no helical content at pH 8.5 does not mean that it remains extended without structure. In fact, it is not so unusual that the peptide forms transient *turn* and *bend* structures (Figure 3). Figure 2b shows the number of helical residues at pH 11.5 and ionic strength 0.0 M. In contrast with plot a, the peptide is in this case adopting the helical form almost exclusively (see Figure 1). As a consequence, only a very brief loss of structure is observed around 11 ps.

The reverse of an helix−coil transition is the helix formation, which is in direct relation with protein folding. Throughout our simulations we observed several refoldings in the time scale used. For example, in Figure 2a, we observed a complete refolding of the structure at around 11 ns, which is transient due to the low pH value of the simulation.

Helix−Coil Transition. Chou and Scheraga[47] reported, using optical rotatory dispersion (ORD), that, at 25 °C in water, the helix-to-coil transition occurs at pH 10.3, when the polymer (∼670 Lys residues) is 35% charged. Our results (Figure 4) show a clear transition from helix to coil upon pH decrease. An obvious difference between the experimental and the simulation is the shape of the curve which, in the experimental case, has a very abrupt transition. The increase of abruptness with chain length is actually to be expected, being well-known both experimentally and theoretically,[59] leading to a quasi-phase-transition for very long chains.

The pH at half-transition (∼10.2) for I = 0.1 M is in very good agreement with the experimental one (∼10.3). If we take

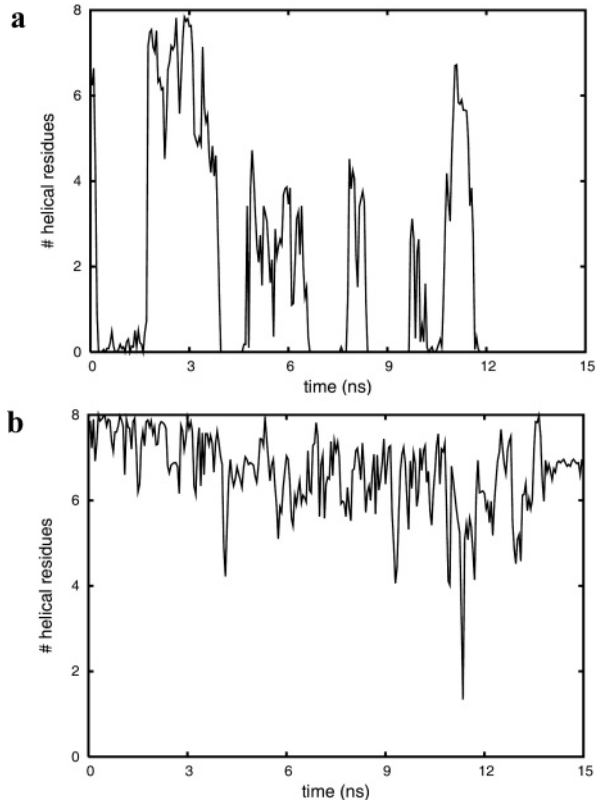

Figure 2. Helical content of decalysine at pH 8.5 (a) and 11.5 (b) and ionic strength 0.0 M (block averages with a block size of 20 × 1 ps).

the pH value obtained here for half-transition and use it in the titration curve of Figure 1, we obtain a value of ∼35% charge, which is in excellent agreement with the experimental results.

The helicity curve for lower ionic strength (I = 0.0 M) is shifted toward lower pH values. This shift can be explained by the difference in the charges between the two ionic strength values at a certain pH (Figure 1).

With the help of the titration curves, we can plot the helicity curves as a function of protonation (Figure 5), which allows for a direct comparison between different ionic strength values and with experimental results. In this figure, we see that the half-transition point at ionic strength 0.1 M occurs at ∼35% protonation for both experimental and simulation, while a value of ∼40% charge is observed at 0.0 M. The fact that the lower ionic strength curve shows a sharper transition has no obvious interpretation. More simulations at different ionic strength values would give better insight into this subject.

Since there is no reason to expect an exact correspondence between the experimental ORD data and the DSSP-derived helical content, alternative helicity measures may be used. A possible measure can be obtained by monitoring H-bond distances over the simulation. In a fully helical decalysine, one can identify 6 hydrogen bonds between the i carbonyl group and the $i + 4$ amide group. The monitoring of these 6 distances can give us an alternative way to follow the helix−coil transition. In Figure 6, we plotted the average distance of these bonds over pH for both ionic strength values. We observe a clear trend in the curves, where the lower distances are associated with the helical structures and the higher distances to the coiled ones. We note that the significantly large values obtained at low pH reflect the presence of fairly extended conformations, which are the ones providing the best solvation for the positively charged chains. If we define the half-transition point to be the average between the maximum distance in our

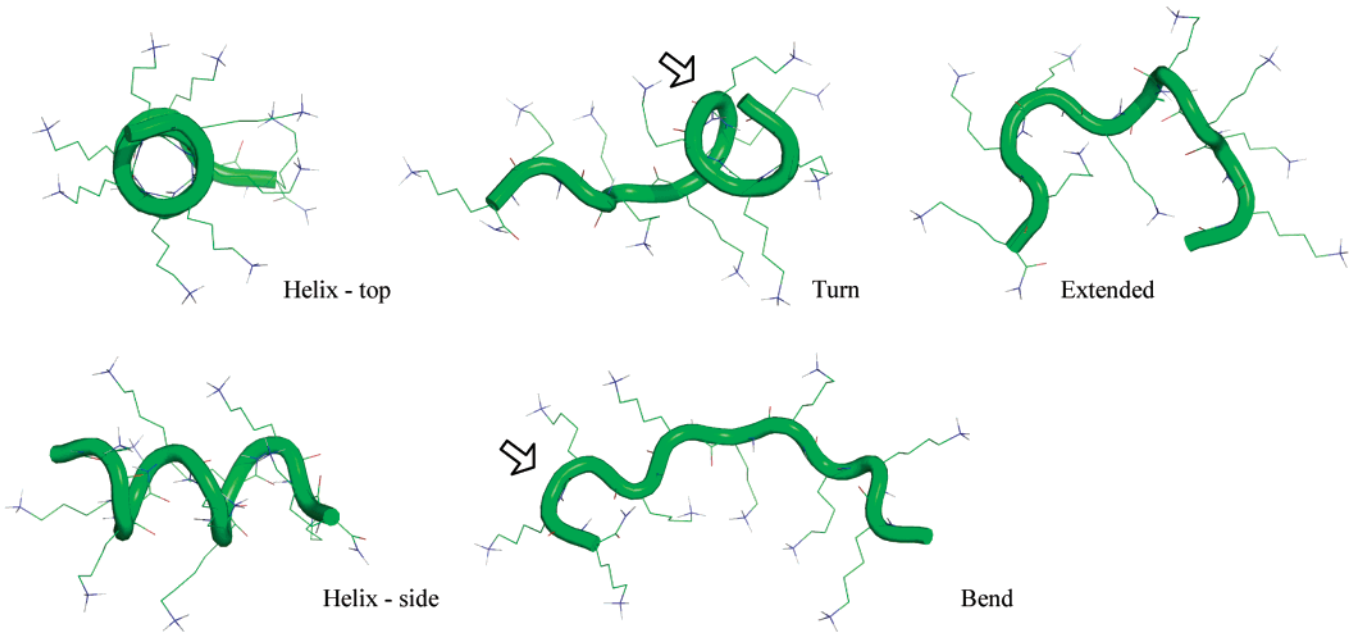

Figure 3. Typical conformations of decalysine at pH 8.5 and ionic strength 0.0 M. Images were done with PyMOL.[58]

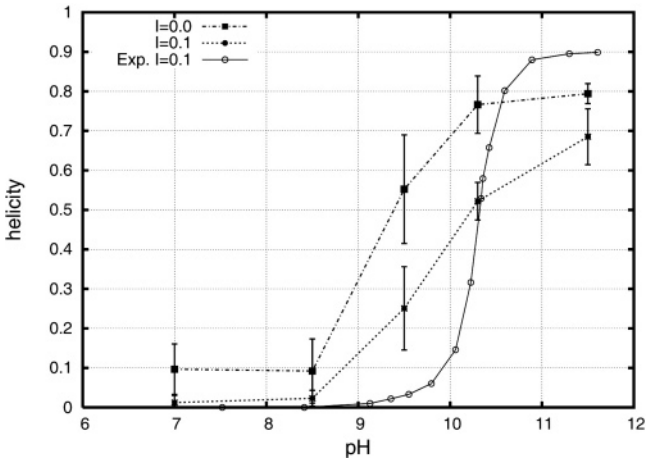

Figure 4. Helicity curves obtained from DSSP (fraction of average helical residues) compared with the experimental results (obtained from ORD data at ionic strength 0.1 M KCl).[47]

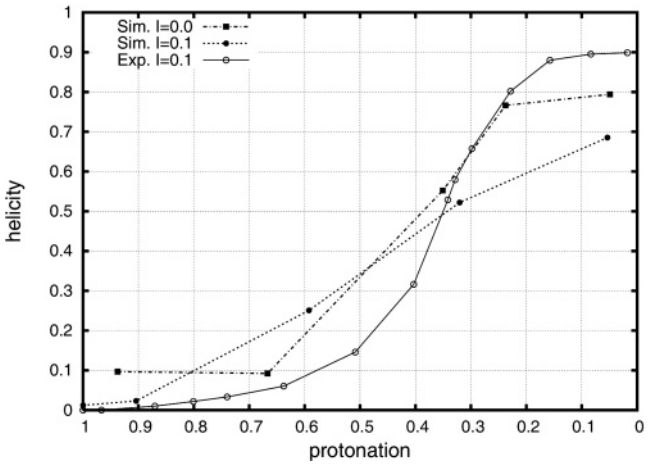

Figure 5. Helicity curves plotted against the deprotonation fraction. The experimental curve was obtained by combining data from Chou and Scheraga.[47]

plot and a value of 3 Å (which is a typical distance for a perfect α-helix), then we obtain from the plot a pH value of ∼10.1, which is in good agreement with the DSSP curves and the experimental data. In this figure, it is also clear that a decrease of ionic strength shifts the transition curve toward lower pH values.

Counterions. As discussed in the Introduction, we modeled counterion effects not by the explicit inclusion of counterions but rather by specifying the ionic strength value in the PB calculations and in the reaction field parameters. As explained there, this choice is motivated by the observation that reaction-field simulations without counterions seem to perform as well as lattice-sum simulations with counterions[45] and from the fact that the total charge is not constant in our constant-pH MD simulations. Nonetheless, we present in this section a comparison between three possible approaches: reaction field without counterions (our standard setup); reaction field with counterions; PME with counterions. All simulations refer to pH 10.3 and ionic strength 0.1 M. We expect this to be a rather stringent test, because at this pH value the decalysine molecule displays large fluctuations of conformation and of protonation states. The simulations with explicit counterions included 2 Na^+ and 5 Cl^-.

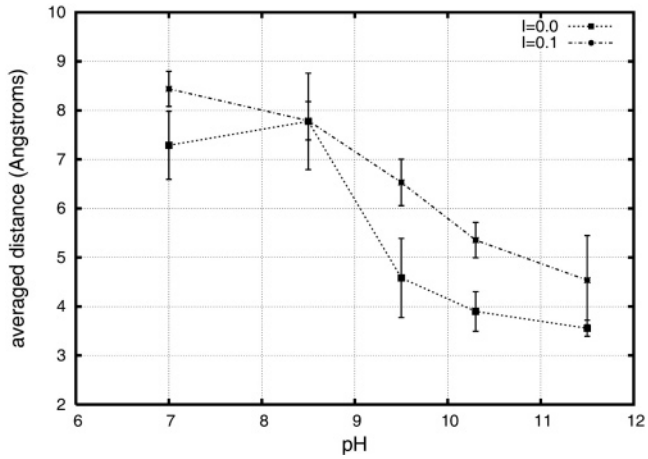

Figure 6. Average H-bond distance obtained at each pH value.

These charges allow both for a close neutralization of the system (at pH 10.3 approximately 3 Lys residues are charged on average) and for a total ion concentration around 0.1 M. The simulation using the reaction field was severely affected by the

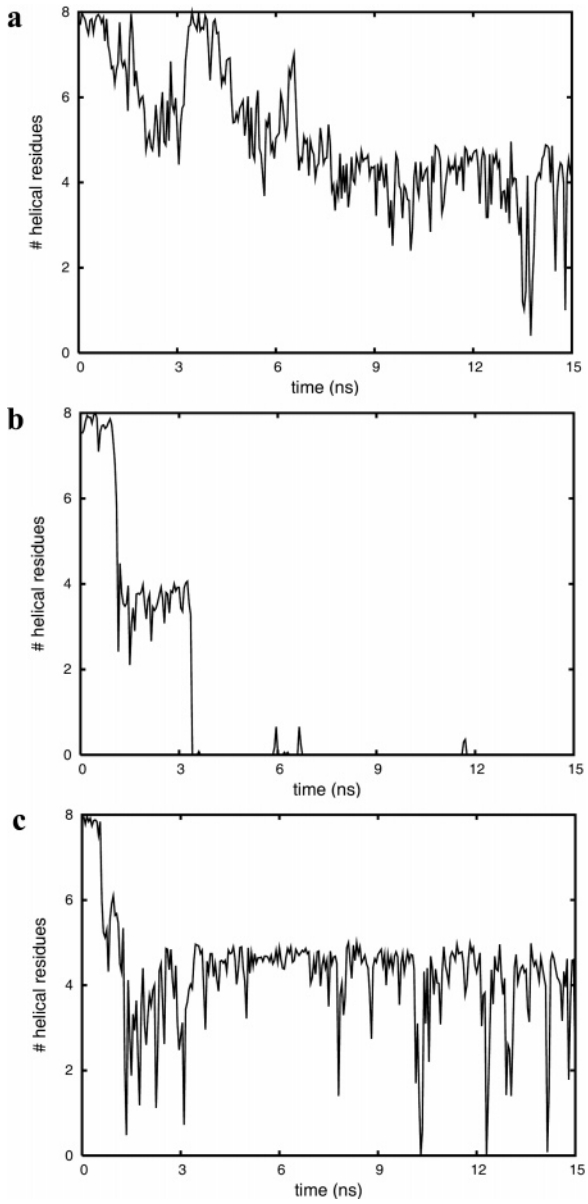

Figure 7. Helical content of decalysine at pH 10.3 and ionic strength 0.1 M (block averages with a block size of 20 × 1 ps): (a) reaction field without ions; (b) reaction field with ions; (c) PME with ions.

introduction of ions. After 3 ns, the decalysine helix completely unfolds and remained a coil throughout the rest of the simulation (Figure 7b). On the other hand, in the simulation using PME, the decapeptide behaved in excellent agreement with our results without counterions (Figure 7a,c). This agreement between both methodologies strongly suggests that the one adopted in this study is a sound one. Furthermore, these results open the possibility of using the constant-pH MD method with PME dealing with the long-range electrostatic interactions. But, although the approximate neutralization does not seem to have deleterious effects on the PME algorithm, there is the obvious drawback of having to know in advance the amount of charge that neutralizes the system at each pH value.

Conclusions

In terms of methodology, this work presents a new implementation of the stochastic titration method for constant-pH MD.[32] The major novelty is the inclusion of ionic strength effects, which is obtained by specifying the ionic strength value in the PB calculations, as well as in the reaction field parameters; this approach does not use explicit counterions, being supported by a posteriori comparisons with PME simulations using approximate charge neutralization. Furthermore, a faster MD algorithm (GROMACS) is used and the effect of protonation events is fully included in the force field parameters (instead of the simple charge modification previously used). An efficient reduced titration treatment is also implemented, which prevents unnecessary PB calculations.

The application of the method to a decalysine peptide shows very good agreement with experiments performed on poly-L-lysine at an ionic strength of 0.1 M.[47] The overall trend of the helix−coil transition induced by pH is reproduced, and the pH values corresponding to midpoint titration and midpoint helix−coil transition show excelent agreement with experiments. Our results for ionic strength 0.0 M show a shift of the protonation and helix−coil transition curves toward lower pH (around 1 pH unit), revealing that ionic strength effects can be significant. Interestingly, our results for 0.0 M are very similar to those obtained in the decalysine simulations performed by Börjesson and Hünenberger using the acidostat method,[39] which does not take ionic strength effects into account.

Overall, the present results suggest that our stochastic titration method for constant-pH MD simulations can properly model the coupling between protonation and conformation in a large peptide, as well as its dependence on ionic strength. This gives good prospect for its application in the study of protein secondary structure changes leading to misfolding, especially the cases where the loss of helical content upon pH changes is in direct association with disease.[60,61]

Acknowledgment. We thank Cláudio Soares for helpful discussions, and we acknowledge financial support from the Fundação para a Ciência e Tecnologia of Portugal through Grants SFRH/BPD/14540/2003 and POCTI/BME/45810/2002.

References and Notes

(1) Stryer, L. *Biochemistry*, 4th ed.; Freeman: New York, 1995.
(2) Yates, C. M.; Butterworth, J.; Tennant, M. C.; Gordon, A. *J. Neurochem.* **1990**, *55*, 1624.
(3) Hornemann, S.; Glockshuber, R. *Proc. Natl. Acad. Sci. U.S.A.* **1998**, *95*, 6010.
(4) Kelly, J. W. *Proc. Natl. Acad. Sci. U.S.A.* **1998**, *95*, 930.
(5) Warwicker, J.; Watson, H. C. *J. Mol. Biol.* **1982**, *157*, 671.
(6) Sharp, K. A.; Honig, B. *Annu. Rev. Biophys. Biophys. Chem.* **1990**, *19*, 301.
(7) Bashford, D.; Karplus, M. *Biochemistry* **1990**, *29*, 10219.
(8) Yang, A.-S.; Gunner, M. R.; Sampogna, R.; Sharp, K.; Honig, B. *Proteins: Struct. Funct. Genet.* **1993**, *15*, 252.
(9) Simonson, T. *Curr. Opin. Struct. Biol.* **2001**, *11*, 243.
(10) Bashford, D. *Front. Biosci.* **2004**, *9*, 1082.
(11) Bashford, D.; Case, D. A. *Annu. Rev. Phys. Chem.* **2000**, *51*, 129.
(12) Feig, M.; Brooks, C. L., III. *Curr. Opin. Struct. Biol.* **2004**, *14*, 217.
(13) Lee, F. S.; Chu, Z. T.; Warshel, A. *J. Comput. Chem.* **1993**, *14*, 161.
(14) Sham, Y. Y.; Chu, Z. T.; Warshel, A. *J. Phys. Chem. B* **1997**, *101*, 4458.
(15) Antosiewicz, J.; Porschke, D. *Biochemistry* **1989**, *28*, 10072.
(16) Beroza, P.; Fredkin, D. R.; Okamura, M. Y.; Feher, G. *Proc. Natl. Acad. Sci. U.S.A.* **1991**, *88*, 5804.
(17) Baptista, M.; Martel, P. J.; Soares, C. M. *Biophys. J.* **1999**, *76*, 2978.
(18) Tanford, C.; Roxby, R. *Biochemistry* **1972**, *11*, 2192.
(19) Gilson, M. K. *Proteins: Struct. Funct. Genet.* **1993**, *15*, 266.
(20) Spassov, V.; Bashford, D. *J. Comput. Chem.* **1999**, *20*, 1091.
(21) Bashford, D.; Karplus, M. *J. Phys. Chem.* **1991**, *73*, 3488.
(22) Eberini, I.; Baptista, A. M.; Gianazza, E.; Fraternali, F.; Beringhelli, T. *Proteins: Struct. Funct. Bioinf.* **2004**, *54*, 744.
(23) Warshel, A.; Åqvist, J. *Annu. Rev. Biophys. Biophys. Chem.* **1991**, *20*, 267.
(24) Sham, Y. Y.; Muegge, I.; Warshel, A. *Biophys. J.* **1998**, *74*, 1744.

(25) Simonson, T.; Archontis, G.; Karplus, M. *J. Phys. Chem. B* **1999**, *103*, 6142.
(26) Warshel, A.; Sussman, F.; King, G. *Biochemistry* **1986**, *25*, 8368.
(27) Jorgensen, W. L.; Briggs, J. M. *J. Am. Chem. Soc.* **1989**, *111*, 4190.
(28) Schutz, C. N.; Warshel, A. *Proteins: Struct. Funct. Genet.* **2001**, *44*, 400.
(29) Archontis, G.; Simonson, T. *Biophys. J.* **2005**, *88*, 3888.
(30) Mertz, J. E.; Pettitt, B. M. *Int. J. Supercomput. Appl.* **1994**, *8*, 47.
(31) Baptista, A. M.; Martel, P. J.; Petersen, S. B. *Proteins: Struct. Funct. Genet.* **1997**, *27*, 523.
(32) Baptista, A. M.; Teixeira, V. H.; Soares, C. M. *J. Chem. Phys.* **2002**, *117*, 4184.
(33) Walczak, A. M., Antosiewicz, J. M. *Phys. Rev. E* **2002**, *66*, 051911.
(34) Dlugosz, M.; Antosiewicz, J. M.; Robertson, A. D. *Phys. Rev. E* **2004**, *69*, 021915.
(35) Dlugosz, M.; Antosiewicz, J. M. *Chem. Phys.* **2004**, *302*, 161.
(36) Mongan, J.; Case, D. A.; McCammon, J. A. *J. Comput. Chem.* **2004**, *25*, 2038.
(37) Bürgi, R.; Kollman, P. A.; van Gunsteren, W. F. *Proteins: Struct. Funct. Genet.* **2002**, *47*, 469.
(38) Börjesson, U.; Hünenberger, P. H. *J. Chem. Phys.* **2001**, *114*, 9706.
(39) Börjesson, U.; Hünenberger, P. H. *J. Phys. Chem. B* **2004**, *108*, 13551.
(40) Baptista, A. M. *J. Chem. Phys.* **2001**, *116*, 7766.
(41) Lee, M. S.; Salsbury Jr., F. R.; Brooks, C. L., III. *Proteins: Struct. Funct. Bioinf.* **2004**, *56*, 738.
(42) Khandogin, J.; Brooks, C. L., III. *Biophys J.* **2005**, *89*, 141.
(43) Kong, X.; Brooks, C. L., III. *J. Chem. Phys.* **1996**, *105*, 2414.
(44) Ibragimova, G. T.; Wade, R. C. *Biophys. J.* **1998**, *74*, 2906.
(45) Walser, R.; Hünenberger, P. H.; van Gunsteren, W. F. *Proteins: Struct. Funct. Genet.* **2001**, *44*, 509.
(46) Tironi, I. G.; Sperb, R.; Smith, P. E.; van Gunsteren, W. F. *J. Chem Phys.* **1995**, *102*, 5451.
(47) Chou, P. Y.; Scheraga, H. A. *Biopolymers* **1971**, *10*, 657.
(48) Berendsen, H. J. C.; van der Spoel, D.; van Drunen, R. *Comput. Phys. Commun.* **1995**, *91*, 43.
(49) Bashford, D.; Gerwert, K. *J. Mol. Biol.* **1992**, *224*, 473.
(50) Gilson, M. K.; Sharp, K. A.; Honig, B. *J. Comput. Chem.* **1987**, *9*, 327.
(51) Oostenbrink, C.; Villa, A.; Mark, A. E.; van Gunsteren, W. F. *J. Comput. Chem.* **2004**, *25*, 1656.
(52) Hermans, J.; Berendsen, H. J. C.; van Gunsteren, W. F.; Postma, J. P. M. *Biopolymers* **1984**, *23*, 1513.
(53) Hess, B.; Bekker, H.; Berendsen, H. J. C.; Fraaije, J. G. E. M. *J. Comput. Chem.* **1997**, *18*, 1463.
(54) Berendsen, H. J. C.; Postma, J. P. M.; van Gunsteren, W. F.; DiNola, A.; Haak, J. R. *J. Chem. Phys.* **1984**, *81*, 3684.
(55) Darden, T. A.; York, D. M.; Pedersen, L. *J. Chem. Phys.* **1993**, *98*, 10089.
(56) Kabsch, W.; Sander, C. *Biopolymers* **1983**, *22*, 2577.
(57) Allen, M. P.; Tildesley, D. J. *Computer Simulations of Liquids*; Oxford University Press: New York, 1987.
(58) DeLano, W. L. *The PyMOL Molecular Graphics System*; DeLano Scientific: San Carlos, CA, 2002; http://www.pymol.org.
(59) Poland, D.; Scheraga, H. A. *Theory of Helix-Coil Transitions in Biopolymers*; Academic Press: New York, 1970.
(60) Pan, K. M.; Baldwin, M.; Nguyen, J.; Gasset, M.; Serban, A.; Groth, D.; Huang, Z.; Fletterick, R. J.; Cohen, F. E.; Prusiner, S. B. *Proc. Natl. Acad. Sci. U.S.A.* **1993**, *90*, 10962.
(61) Safar, J.; Roller, P. P.; Gajdusek, D. C.; Gibbs, C. J., Jr. *Protein Sci.* **1993**, *2*, 2206.